



Biosynthesis of Zinc Oxide Nanoparticles and Their Evaluation for Wound Healing Application Using NIH-3T3 Fibroblast Cell Line

SHRAVANI RAMESH WADEKAR^{1*}, MANISH SHAMRAO HATE¹
and RAMESH CHAUGHULE²

¹Department of Chemistry, Ramnarain Ruia Autonomous College, L.N. Road, Matunga (East), Mumbai-400019, India.

²Ex. Tata Institute of Fundamental Research, Mumbai, India, Adjunct Professor, Ramnarain Ruia Autonomous College, Mumbai, India.

*Corresponding author E-mail: shravaniwadekar996@gmail.com

<http://dx.doi.org/10.13005/ojc/410505>

(Received: May 02, 2025; Accepted: September 12, 2025)

ABSTRACT

This study investigates the wound healing potential of biosynthesized zinc oxide nanoparticles (ZnO NPs) using a scratch assay on non-cancerous NIH-3T3 fibroblast cells. The ZnO NPs were synthesized using *Cassia fistula* leaf extract and previously characterized by UV-Visible Spectroscopy, FTIR, PXRD, FESEM, and HRTEM. The hexagonal wurtzite structure, which had an average crystalline size of 14.91 nm, was confirmed by XRD analysis. Prior research demonstrated their biocompatibility, with an IC_{50} value of 38.56 $\mu\text{g/mL}$ as determined by the MTT assay. Building on these findings, the current study evaluates the effect of ZnO NPs on fibroblast migration, a critical step in the wound healing process. The scratch assay showed a 4.30% cell migration rate on day one lower than control group (23.20%), higher than commercial ZnO (1.61%) in a single run experiment, indicating enhance cell mobility of ZnO NPs while maintaining controlled cytotoxicity. These findings highlight the features of biosynthesized ZnO NPs as a sustainable and economical wound healing material. However, additional investigations with triplicates, *in vivo* (animal model) studies, and clinical trials with statistical validation are necessary to ascertain reliability and practical application. Thus, this study establishes the groundwork for eco-friendly ZnO NPs in biomedical applications, specifically in wound treatments.

Keywords: *Cassia fistula*, ZnO NPs, NIH-3T3 fibroblast cells (non-cancerous), MTT assay, Scratch assay, Migration rate.

INTRODUCTION

Wound healing is a multifaceted and dynamic biological process that encompasses haemostasis, inflammation, proliferation, and

tissue remodelling¹. Skin tissue regeneration has been a crucial study topic in recent years because of the difficulties in restoring injured tissue. The human body depends on the skin as a principal barrier against dust, debris, toxic



substances, and other environmental factors. Nonetheless, when the integument is impaired owing to burns, trauma, surgical interventions, infections, or diabetic ulcers, the mechanism of tissue regeneration becomes exceedingly intricate. Tissue repair following injury encompasses complex biological and physiological processes, including inflammation, cellular proliferation, extracellular matrix remodelling, and fibroblast migration to the damaged site².

Fibroblast migration is essential for extracellular matrix deposition, collagen synthesis, and overall tissue repair among various phases³. Damaged fibroblast function can result in delayed healing and persistent wounds, requiring the formulation of innovative treatment approaches to enhance tissue regeneration^{4,5}. ZnO NPs have drawn significant interest in biological research owing to their antibacterial, anti-inflammatory, and regenerative characteristics. Their nanoscale dimensions, elevated surface-to-volume ratio, and distinctive physicochemical characteristics make them intriguing candidates for wound healing applications. Prior research has shown that ZnO NPs may boost cell proliferation, re-epithelialization, and migration, which are essential components of wound healing^{6,7}. ZnO NPs release Zn²⁺ ions in contact with aqueous environments, such as body fluids, cell culture media, or wound exudates. The Zn²⁺ ions facilitate the growth and division of skin cells (keratinocytes and fibroblasts), resulting in proliferation. The proliferation facilitates cellular movement toward the site, thereby promoting successful wound closure and demonstrating cell migration. Additionally, a new skin layer forms at the wound site, facilitating re-epithelialization, enhancing cell adhesion, and accelerating tissue recovery. Their antimicrobial properties also prevent infection and facilitate efficient and rapid wound healing.

However, their cytotoxic effects present an issue, requiring meticulous assessment to guarantee their safe and successful use in regenerative medicine^{8,9}.

The fast release of ZnO NPs (burst out release), leads to elevated concentrations of Zn²⁺ ions, may induce cytotoxicity. Increased levels of

Zn²⁺ ions can generate reactive oxygen species (ROS), leading to oxidative stress and ultimately causing cell death (apoptosis). Thus, utilizing a low concentration of ZnO NPs is an effective method to reduce cytotoxicity and facilitate safe, fast healing. A concentration of 0.01 mg/mL (often below 1 mg/mL) is commonly considered useful for promoting wound healing while minimizing cytotoxicity; thus, a low concentration was chosen to guarantee biocompatibility and therapeutic efficacy¹⁰. Controlled release is crucial, indicating that rapid release (burst) may cause cytotoxicity, and too slow might be ineffective. Showing low initial migration is necessary to prevent irritation or toxicity. Thus, gradual, sustained release over time is essential to support healing over several days.

In our previous study, we synthesized ZnO NPs using *Cassia fistula* leaf extract and analysed them through UV-Visible spectroscopy, FTIR, PXRD, FESEM, HRTEM, and EDAX1. The MTT assay and cytotoxicity evaluation showed an IC₅₀ value of 38.56 µg/mL for 0.001 mg/mL ZnO NPs, thereby defining a safe concentration range for subsequent biological investigations. The cytotoxicity evaluation using the MTT assay showed an IC₅₀ value of 38.56 µg/mL for 0.001 mg/mL ZnO NPs, thereby defining a safe concentration range for subsequent biological investigations¹¹.

This study seeks to examine the wound-healing efficacy of ZnO NPs by a scratch assay conducted on NIH-3T3 fibroblast (non-cancerous) cells. The scratch assay is a recognized *in-vitro* technique for evaluating cell migration, a crucial component of the wound healing process. This study examines the impact of ZnO NPs on fibroblast migration, elucidating their function in facilitating wound closure and enhancing tissue restoration.

Mechanism of Fibroblast Response Modulated by ZnO NPs

Figure 1 depicts the cytotoxic effects of ZnO NPs on a fibroblast cell line. Initially, ZnO NPs interact with the cell membrane, causing breakage and enabling the penetration and release of Zn²⁺ ions into the surrounding environment.

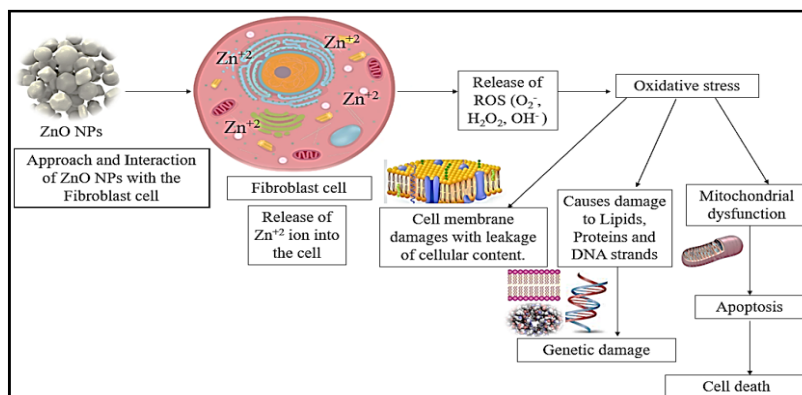


Fig. 1. Schematic representation of the biological pathway for the cytotoxic effects of ZnO NPs on fibroblast cell lines, adapted from Singh, S. (2018). Zinc oxide nanoparticles impact: cytotoxicity, genotoxicity, developmental toxicity, and neurotoxicity. *Toxicology Mechanisms and Methods*, 29(4), 300–311. <https://doi.org/10.1080/15376516.2018.1553221>

The Zn²⁺ ions facilitate the intracellular release of reactive oxygen species (ROS), including superoxide (O₂⁻), hydrogen peroxide (H₂O₂), and hydroxyl anions (OH⁻). Oxidative stress results from an imbalance between the generation of reactive oxygen species (ROS) and the capacity of defence against antioxidants. It can be recognized as a signalling molecule that mediates between cell survival and cell death. The formation and rise of reactive oxygen species (ROS) within the cell ultimately result in oxidative damage to cellular components, impairing the cellular system. Reactive oxygen species (ROS) produce oxidative stress in cells, leading to the rupture of cell membranes and significant damage to lipids, proteins, and DNA strands, ultimately causing genetic damage. The elevated oxidative stress also impairs mitochondrial function, hence enhancing apoptotic signalling. The formation of oxidative stress by ZnO NPs exhibits a dual nature; under low and controlled conditions, it may benefit cells; however, at elevated levels, it can induce cytotoxicity due to reactive oxygen species generation and cellular malfunction¹²⁻¹⁴.

MATERIALS AND METHODS

Synthesis of ZnO NPs: ZnO NPs were synthesized according to the previously reported protocol using *Cassia fistula* leaves extract and the synthesized ZnO NPs were subjected to hyphenated analytical techniques including UV-Vis, FTIR, PXRD, FESEM, HRTEM and EDAX, as reported earlier¹.

Cell culture setup: The NIH-3T3 mouse fibroblast cell line was obtained from the National Fungal Culture Collection of India (NFCCI) at the

Agharkar Research Institute in Pune, was utilized to assess cell migration rates via a scratch assay. Sterile 10 µL pipette tips (for making scratch), sterile 6-well tissue culture plate, CO₂ incubator and test samples as Positive control (cells treated with 0.001 mg/mL of ZnO NPs and 0.001 mg/mL of commercial ZnO) and negative control (untreated cells) were employed to analyse comparative experimental outcomes.

Cell growth medium reagents: DMEM (Dulbecco's Modified Eagle Medium), PBS (Phosphate buffer saline), L-glutamine and sodium pyruvate along with 10% penicillin streptomycin solution for cell maintenance, all obtained from Sigma-Aldrich, Mumbai, India, of 98 percent purity with CAS number 50-99-7 of A.R. grade. All test specimens were freshly prepared in a medium prior to application under completely sterile conditions.

Scratch assay

Sample preparation: The lowest concentration (0.01 mg/mL) of ZnO NPs and commercial ZnO samples were subjected to sonication for one hour prior to application to the cells for treatment. The medium and reagents were sterilized using 0.22 µm syringe filters in a laminar flow hood to maintain sterile conditions.

Test cell line: nih 3t3 cells (mouse fibroblast cells) Protocol

After revival, 0.05 million NIH-3T3 fibroblast cells were inoculated into each well of a 6-well plate containing complete growth media. The cells were cultured overnight at 37°C in a humidified 5% CO₂ environment to facilitate optimal adhesion and growth until achieving 100% confluence. Upon achieving

confluence, a meticulous incision was executed across the cell monolayer utilizing a sterile 10 μL pipette tip. The previous culture media was thereafter aspirated gently, and the wells were washed with phosphate-buffered saline (PBS) to eliminate cellular debris. Subsequently, fresh growth medium was introduced to each well. Experimental and control samples were placed into their designated wells. The experimental group consists of 5 μg per 2 mL of 0.01 mg/mL ZnO NPs and 5 μg per 2 mL of 0.01 mg/mL commercial ZnO as a positive control, with untreated cells in regular media serving as the negative control. Before utilization, the ZnO NP samples were subjected to sonication for one hour at 27°C to achieve uniform dispersion and inhibit agglomeration, hence enhancing their contact with cells. The plates were subsequently placed back in the CO₂ incubator, and cell migration over the scratch region was seen under a microscope at 0, 24, 48, and 72 hours. The wound closure rate in the treated groups was compared to the control, establishing a baseline for assessing the wound healing efficacy of ZnO NPs and commercial ZnO.

RESULTS

A. Evaluation of cell migration in wound healing models using the scratch assay

The scratch assay for the wound healing process in samples subjected to control, 0.001 mg/mL of ZnO NPs, and commercial ZnO for a duration of zero, 24 h, 48 h, and 72 h (Fig. 2). Usually, this study aims to investigate various compounds affecting the healing process of wounds through cell proliferation.

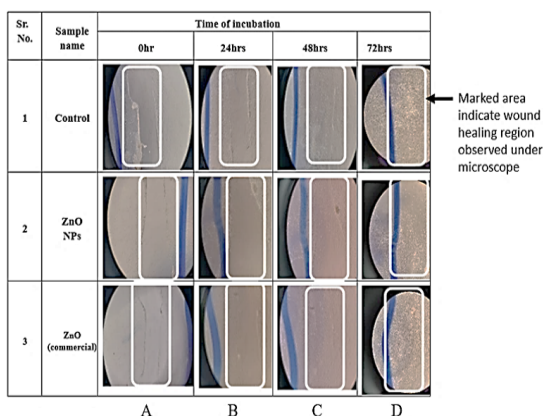


Fig. 2. Microscopic images for wound healing using NIH 3T3 cell line captured at different intervals of time using control, (0.001mg/mL) ZnO NPs and (0.001 mg/mL) ZnO commercial across (A), (B), (C), and (D) with marked area indicating cell migration

At 0 h (Fig. 2A), the wound area established a baseline, indicating the untreated condition of the cell monolayer. This state acted as a benchmark to assess the impact of ZnO NPs and commercial ZnO on wound closure over time. Within 24 h (Fig. 2B), all groups displayed initial symptoms of wound closure, signifying the commencement of the healing process. The group that contained ZnO NPs showed better cell arrangement and movement towards the wound compared to the commercial ZnO and untreated groups. At 48 h (Fig. 2C), the advancement of healing was more pronounced, especially in the ZnO-treated wells, where cells seemed to have migrated more equally into the wound region. After 72 h (Fig. 2D), the ZnO NP group exhibited a well-organized closure pattern with uniform cellular coverage¹⁵. Although commercial ZnO seemed to promote faster covering, the healing in this group was markedly dense and rapid. The control group exhibited irregular migration with partial closure. These data substantiate the wound healing efficacy of biosynthesized ZnO NPs, indicating a consistent and biocompatible healing response^{16,17}.

Migration Study

Cell migration is the movement of cells from their original location to the site of injury, guided by chemical signals (chemotaxis), mechanical cues, and extracellular matrix (ECM) interactions^{18,19}.

Fibroblast cells migrate into the wound site to produce collagen and ECM components. Disruption in cell migration can lead to delayed or chronic wounds, commonly seen in conditions like diabetes²⁰⁻²². The data presented here (Table 1) illustrate cell migration percentages over three days for the ZnO NPs, commercial ZnO, and control groups using 0.001 mg/mL concentration.

Table 1: Percentage cell migration observed for ZnO NPs, ZnO (commercial), and controlled samples for NIH-3T3 Cells (Mouse fibroblast cell line)

Materials	Day 1 %Migration	Day 2 %Migration	Day 3 %Migration
ZnO NPs	4.30	58.04	75.90
ZnO (commercial)	1.61	66.09	98.62
Control	23.20	67.69	91.91

On Day 1, the migration rate for ZnO NP-treated cells was 4.30%, which was lower than the control group (23.20%) but higher than the commercial ZnO group (1.61%), indicating an early stage of biocompatibility. On Day 2, the ZnO NP group demonstrated 58.04% migration, reflecting a consistent improvement in cellular motility, while still somewhat lower than the control (67.69%) and commercial ZnO (66.09%). On Day 3, ZnO NPs facilitated a migration rate of 75.90%, indicating sustained enhancement of tissue regeneration. Conversely, the commercial ZnO attained an impressive value of 98.62%,

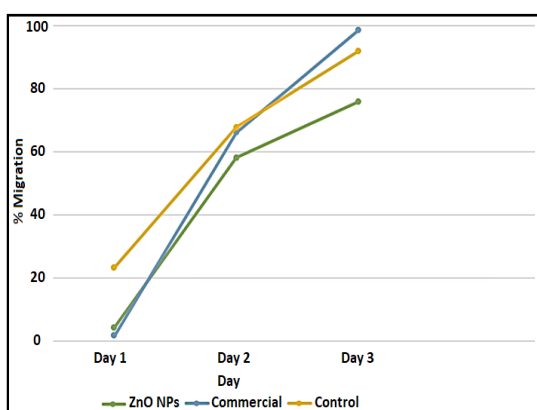


Fig. 3. Indicates the percentage migration rate of ZnO NPs, commercial ZnO, and control samples on Day 1, Day 2 and Day 3 respectively

In wound healing experiments, the opposite trend is generally expected compared to cytotoxicity or anticancer studies. As the concentration increased to 0.01 mg/mL, the toxicity of commercial ZnO exceeded that of ZnO NPs. In summary, ZnO NPs exhibited lower toxicity than commercial ZnO at a concentration of 0.001 mg/mL, hence enhancing cell viability and facilitating cell proliferation^{26,27}. These results align with the scratch assay findings, indicating that ZnO NPs exhibited enhanced wound healing and cell migration at the optimal dose. This corresponds with the idea that reduced toxicity facilitates enhanced cellular mobility and proliferation²⁸. Consequently, ZnO NPs exhibited optimal outcomes at a concentration of 0.001 mg/mL, where cell viability was maximized and wound healing was most efficacious. With the rise in concentration, toxicity escalated, leading to diminished viability and reduced migratory rates. The % viabilities for concentrations of 5 μ g/mL and 10 μ g/mL of 0.001 mg/mL of ZnO NPs sample reported in our earlier publication against fibroblast

while the control achieved 91.91%. Therefore, commercial ZnO had the highest proliferation rate, followed by the control and ZnO NPs²³⁻²⁵. Therefore, altering size, surface-to-volume ratio, and concentration can improve their reactivity rate (Table 1) and the graph showing corresponding values are shown in Figure 3.

Correlation between scratch assay and mtt assay

ZnO NPs demonstrated superior cell viability and reduced toxicity at a concentration of 0.001 mg/mL compared to commercial ZnO at the identical dose¹ in an MTT Assay (Figure 4).

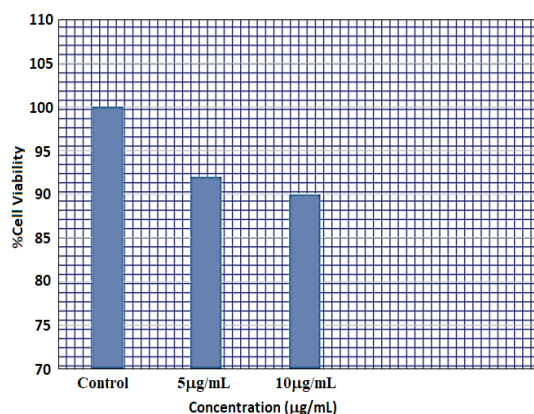


Fig. 4. Evaluation of Cell Viability Across Varying Concentrations of 0.001 mg/mL ZnO NPs

cells are 92.019% and 90.003% respectively, as against 100 % viability¹. These differences in cell behaviour may be due to well conditions or changes in oxygenation or nutrient availability, affecting fibroblast cells behaviour and sensitivity²⁹. Volumes of the samples do not play any role in the % viability of fibroblast cells. Minimizing sample volumes is preferable to prevent harm to live cells.

DISCUSSION

In wound healing and regenerative medicine, enhanced fibroblast migration is desirable, as it significantly contributes to tissue repair³⁰. The higher migration rate observed with biosynthesized ZnO NPs suggests better biocompatibility, bioactivity, and more favourable surface properties that interact positively with cells³¹. Notably, the fibroblast migration achieved with commercial ZnO (1.61%) was less than half of that observed with biosynthesized ZnO NPs (4.30%), indicating the superior cell-stimulating potential of the biosynthesized form, which could be

more effective for biomedical and wound healing applications³². Normal cells maintain higher viability, thus supporting the material's biocompatibility and safety, as confirmed by toxicity experiments³³. The elevated cell migration percentage (4.30% on day 1) for ZnO NPs treated group was associated with increased cell migration, suggesting enhanced wound healing capacity. This difference in performance could be attributed to factors such as particle size, surface charge, morphology, and the presence of phytochemicals from the green synthesis as suggested by previous studies¹, which may enhance the interaction between biosynthesized ZnO NPs and cell membranes. In contrast, commercially synthesized ZnO, often produced through physical or chemical routes, may lack such bioactive surface characteristics.

The biosynthesis of ZnO NPs was carried out using *Cassia fistula* (Bahava) leaf extract, following a previously reported method¹. The plant extract, abundant in phytochemicals, is crucial in nanoparticle synthesis by autonomously reducing metals to metal oxide nanoparticles and stabilizing them, so obviating the necessity for external chemical agents. The resultant ZnO NPs were characterized by UV-Vis spectroscopy, FTIR, PXRD, FESEM, HRTEM, and EDAX, confirming their crystalline structure, purity, and morphology as detailed in our earlier study¹. The ZnO NPs were then evaluated for their impact on fibroblast migration using the scratch assay over a three-day period, in comparison with commercial ZnO and untreated control cells. MTT assay results indicated that commercial ZnO exhibited significantly higher cytotoxicity compared to biosynthesized ZnO NPs. The rapid wound closure associated with commercial ZnO may not represent proper tissue regeneration but could rather be a compensatory response by stressed and impaired cells. Under hazardous conditions, cells often exhibit a "panic response," migrating quickly to maintain tissue integrity, although they may not remain viable or functionally unstable. Conversely, biosynthesized ZnO NPs at an optimal concentration of 0.001 mg/mL promoted elevated cell viability and regulated, healthy migration, aligning with a non-toxic and regenerative healing mechanism. However, at higher concentrations (0.1 mg/mL), ZnO NPs induced oxidative stress, which is mostly due to direct interactions with the cell membrane and the subsequent production of reactive oxygen

species (ROS), leading to mitochondrial dysfunction and apoptosis³⁴. Thus, the combined evaluation of ion release and cellular response confirms that biosynthesized ZnO NPs, when used at appropriate concentrations, offer a safer and more effective alternative for wound healing compared to their commercial counterparts.

The findings indicate insights into the wound healing capacity of ZnO NPs through migration experiments; nevertheless, some limitations must be acknowledged, which can be addressed by additional validations. Future investigations will validate the statistical analysis to reinforce the observed pattern. Future research will involve biological (triplicates) *in-vivo* experimental setup and statistical validation (eg., ANOVA or t-test) of cell proliferation to elucidate the role of ZnO NPs in wound closure³⁵.

CONCLUSION

The migratory behaviour of biosynthesized ZnO NPs, commercial ZnO, and control samples was assessed over three days to evaluate their wound healing potential. Biosynthesized ZnO NPs induced higher fibroblast migration on Day 1 (4.30%), supporting early tissue repair, while maintaining a steady, controlled increase by Day 3 (75.90%), suggesting safer and sustained healing. In contrast, commercial ZnO showed an abrupt surge in migration by Day 3 (98.62%), indicating a risk of oxidative stress due to sudden ion release. The control group exhibited irregular migration, raising concerns about unregulated healing. The *Cassia fistula*-mediated ZnO NPs demonstrated superior biocompatibility, likely due to eco-friendly synthesis without chemical stabilizers. Overall, the biosynthesized ZnO NPs present a promising, natural alternative for wound healing, warranting further optimization for clinical applications.

These promising results underscore the promise of biosynthesized ZnO NPs as a safe and efficacious wound healing remedy. To validate these findings and comprehensively assess their therapeutic potential, further investigations will emphasize statistical validation and incorporate cell proliferation assays. Subsequent investigations utilizing *in vivo* models (triplicate experimental setup) and clinical trials will be crucial for evaluating the

practical implementation of these nanoparticles in wound management. Examining and mitigating potential dangers linked to the abrupt release of ions from commercial ZnO will also be a primary emphasis. Optimizing the synthesis, dose, and delivery strategies can maximize the clinical viability of biosynthesized ZnO NPs.

ACKNOWLEDGEMENT

The authors sincerely express their gratitude to Dr. P.S. Ramanathan's laboratory

at Ramnarain Ruia Autonomous College for their support. Special thanks to the Institute of Chemical Technology (ICT), Matunga; the Indian Institute of Technology (IIT) Mumbai; the National Facility for Biopharmaceuticals (NFB) at Khalsa College, Matunga; and ICON Labs, Navi Mumbai, for their valuable assistance in characterization and data analysis.

Conflict of interest

The authors hereby declare that there is no conflict of interest among themselves.

REFERENCES

- Wadekar, S. R.; Hate, M. S.; & Chaughule, R., *Orient. J. Chem.*, **2024**.
- Dam, P.; Celik, M.; Ustun, M.; Saha, S.; Saha, C.; Kacar, E.A.; Kugu, S.; Karagulle, E. N.; Tasoglu, S.; Buyukserin, F.; Mondal, R.; Roy, P.; Macedo, M. L. R.; Franco, O. L.; Cardoso, M. H.; Altuntas, S.; & Mandal, A. K., *RSC Advances.*, **2023**, 13(31), 21345–21364.
- Khatami, M.; Varma, R. S.; Zafarnia, N.; Yaghoobi, H.; Sarani, M.; & Kumar, V. G., *Sustainable Chemistry and Pharmacy.*, **2018**, 10, 9–15.
- Kumar, S. S. D.; Rajendran, N. K.; Houreld, N. N.; & Abrahamse, H., *International J. of Biological Macromolecules.*, **2018**, 115, 165–175.
- Lau, P.; Bidin, N.; Islam, S.; Shukri, W. N. B. W. M.; Zakaria, N.; Musa, N.; & Krishnan, G., *Lasers in Surgery and Medicine.*, **2016**, 49(4), 380–386.
- Gurunathan, D.; Dinesh, S.; Ramakrishnan, M.; Shanmugam, R., & Missier, M. S., *World Journal of Dentistry.*, **2024**, 15(2), 102–106.
- Naghib, S. M.; Bakhshi, M.; Ahmadi, B.; & Bakhshi, A., *In ACS symposium series.*, **2024**, 221–256.
- Khan, A. U. R.; Huang, K.; Jinzhong, Z.; Zhu, T.; Morsi, Y.; Aldalbahi, A.; El-Newehy, M.; Yan, X., & Mo, X., *Journal of Materials Chemistry B.*, **2021**, 9(5), 1452–1465.
- Hamed, S. H.; Azooz, E. A., & Al-Mulla, E. a. J., *Nano Biomedicine and Engineering.*, **2023**, 15(4), 425–435.
- Escher, B. I.; Henneberger, L.; König, M.; Schlichting, R., & Fischer, F. C., *Environmental Health Perspectives.*, **2020**, 128(7).
- Augustine, R.; Dominic, E. A.; Reju, I.; Kaimal, B.; Kalarikkal, N., & Thomas, S., *RSC Advances.*, **2014**, 4(47), 24777.
- Naskar, A.; & Kim, K., *Pharmaceutics.*, **2020**, 12(6), 499.
- Ravichandran, S.; Paluri, V.; Kumar, G.; Loganathan, K.; & Venkata; B. R. K., *Journal of Experimental Nanoscience.*, **2025**, 11(6), 445–458.
- Saravanakumar, K.; Sathiyaseelan, A.; Zhang, X.; Choi, M.; & Wang, M., *International Journal of Biological Macromolecules.*, **2023**, 242, 124813.
- Bai, D.; Zhang, X.; Zhang, G.; Huang, Y.; & Gurunathan, S., *International Journal of Nanomedicine.*, **2017**, 12, 6521–6535.
- Singh, S., *Toxicology Mechanisms and Methods.*, **2018**, 29(4), 300–311.
- Sezen, S.; Erturk, M. S.; Balpınar, Ö.; Bayram, C.; Özkaraca, M.; Okkay, I. F.; Hacimüftüo lu, A.; & Güllüce, M., *Environmental Science and Pollution Research.*, **2023**, 30(55), 117609–117623.
- Batool, M.; Khurshid, S.; Qureshi, Z.; & Daoush, W. M., *Chemical Papers.*, **2020**, 75(3), 893–907.
- Addis, R.; Cruciani, S.; Santaniello, S.; Bellu, E.; Sarais, G.; Ventura, C.; Maioli, M.; & Pintore, G., *International Journal of Medical Sciences.*, **2020**, 17(8), 1030–1042.
- Asif, N.; Amir, M.; & Fatma, T., *Bioprocess and Biosystems Engineering.*, **2023**, 46(10), 1377–1398.
- Cleetus, C. M.; Primo, F. A.; Fregoso, G.; Raveendran, N. L.; Noveron, J. C.; Spencer, C. T.; Ramana, C. V.; & Joddar, B., *International J. of Nanomedicine.*, **2020**, 15, 5097–5111.
- Chhabra, H.; Deshpande, R.; Kanitkar, M.; Jaiswal, A.; Kale, V. P.; & Bellare, J. R., *RSC Advances.*, **2015**, 6(2), 1428–1439.

23. Heidari, M. K.; Pourmadadi, M.; Yazdian, F.; Rashedi, H.; Ebrahimi, S. a. S.; Bagher, Z.; Navaei Nigjeh, M.; & Haghirosadat, B. F., *Biotechnology Progress.*, **2023**, 39(3).
24. Koupai, A. A.; Varshosaz, J.; Tavakoli, M.; Mirhaj, M.; Salehi, S.; & Dobakhti, F., *Asian J. of Pharmaceutical Sciences.*, **2025**, 10, 1039.
25. Nandhini, J.; Karthikeyan, E.; Sheela, M.; Bellarmin, M.; Kannan, B. G.; Pavithra, A.; Sri, D. S.; Prakash, S. S.; & Kumar, S. R., *Intelligent Pharmacy.*, **2024**.
26. Saghazadeh, S.; Rinoldi, C.; Schot, M.; Kashaf, S. S.; Sharifi, F.; Jalilian, E.; Nuutila, K.; Giatsidis, G.; Mostafalu, P.; Derakhshandeh, H.; Yue, K.; Swieszkowski, W.; Memic, A.; Tamayol, A.; & Khademhosseini, A., *Advanced Drug Delivery Reviews.*, **2018**, 127, 138–166.
27. Vijayakumar, S.; Chen, J.; Kalaiselvi, V.; Tungare, K.; Bhorl, M.; González-Sánchez, Z. I.; & Durán-Lara, E. F., *Environmental Research.*, **2022**, 213, 113655.
28. Ng, C. T.; Yong, L. Q.; Hande, M. P.; Ong, C. N.; Yu, L.; Bay, B. H.; & Baeg, G. H., *International J. of Nanomedicine.*, **2017**, 12, 1621–1637.
29. Abdel-Gawad, D. R.; Shaban, N. S.; Moselhy, W. A.; El-Dek, S.; Ibrahim, M. A.; Azab, A.; & Hassan, N. E. Y., *Journal of Trace Elements in Medicine and Biology.*, **2023**, 81, 127342.
30. Wiesmann, N.; Mendler, S.; Buhr, C. R.; Ritz, U.; Kämmerer, P. W.; & Brieger, J., *Biomedicines.*, **2021**, 9(10), 1462.
31. Wang, J.; Zhang, C.; Xu, X.; Sun, T.; Kong, L.; & Ning, R., *ACS Omega.*, **2024**, 9(52), 51442–51452.
32. Yang, F.; Xue, Y.; Wang, F.; Guo, D.; He, Y.; Zhao, X.; Yan, F.; Xu, Y.; Xia, D.; & Liu, Y., *Bioactive Materials.*, **2023**, 26, 88–101.
33. Tayyeb, J. Z.; Guru, A.; Kandaswamy, K.; Jain, D.; Manivannan, C.; Mat, K. B.; Shah, M. A.; & Arockiaraj, J., *BMC Biotechnology.*, **2024**, 24(1).
34. Nethi, S. K.; Das, S.; Patra, C. R.; & Mukherjee, S., *Biomaterials Science.*, **2019**, 7(7), 2652–2674.
35. Bisht, G.; & Rayamajhi, S., *Nanobiomedicine.*, **2016**, 3.